HAL open science

Blind identification using inverse Patch Transfer Function (iPTF) method

Emmanuel Manu Dabankah, Nicolas Totaro, Jérôme Antoni

To cite this version:

Emmanuel Manu Dabankah, Nicolas Totaro, Jérôme Antoni. Blind identification using inverse Patch Transfer Function (iPTF) method. 23RD INTERNATIONAL CONGRESS ON ACOUSTICS, Sep 2019, Aachen, Germany. hal-02349359

HAL Id: hal-02349359

https://hal.science/hal-02349359v1

Submitted on 5 Nov 2019

HAL is a multi-disciplinary open access archive for the deposit and dissemination of scientific research documents, whether they are published or not. The documents may come from teaching and research institutions in France or abroad, or from public or private research centers.

L'archive ouverte pluridisciplinaire **HAL**, est destinée au dépôt et à la diffusion de documents scientifiques de niveau recherche, publiés ou non, émanant des établissements d'enseignement et de recherche français ou étrangers, des laboratoires publics ou privés.

PROCEEDINGS of the
23rd International Congress on Acoustics

9 to 13 September 2019 in Aachen, Germany

Blind identification using inverse Patch Transfer Function (iPTF) method

Emmanuel Manu DABANKAH[1]; Nicolas TOTARO[1]; Jérôme ANTONI[1]

[1] Univ Lyon, INSA-Lyon, Laboratoire Vibrations Acoustique, F69621 Villeurbanne, France

ABSTRACT

An important object of vibration and noise reduction and control is to identify and localize the vibration and noise sources. Many inverse methods, like Nearfield Acoustic Holography, have been developed in acoustics in the last decades. Among others, the iPTF method, allows the reconstruction of the acoustic fields (pressure, velocity, intensity) directly on the vibrating structure surface even when it has a complex shape. In addition, measurements can be done in non-controlled acoustic environments. The concept of iPTF is based on the application of Green's identity on any closed virtual volume defined around the source. The reconstruction of sound source fields combines discrete acoustic measurements performed at accessible positions around the source with acoustic impedance matrices.

In the present work, blind identification of the vibratory fields is proposed. The "blindness" has here two meanings:

- the identification of the velocity field of a vibrating structure can be blind if obstacles mask parts of the structure to characterize.
- the identification can be blind if the velocity field is the result of the combination of several unknown sources and if one wants to separate the contribution of each source.

Some numerical and experimental results will be shown to illustrate both aspects of the blind identification.

Keywords: acoustic field reconstruction, blind identification, inverse Patch Transfer Function

1. INTRODUCTION

The source identification in the presence of obstacles is a matter of relevance for industrial applications. In automotive industry, it would be valuable to retrieve the velocity field of a source that is intricately located with other structures partially blocking its accessibility. This situation is mostly encountered in the gearbox and engine compartments of a vehicle. In the present study, a method called "inverse Patch Transfer Function" (iPTF) (1-3) is used to handle this task.

The iPTF method is able to identify the vibration velocity of irregularly shaped sources in a non-controlled acoustic environment (reverberant room, stationary disturbing sources, etc.). The objective of this present work is to demonstrate numerically how to use the iPTF method to identify the velocity field of a source masked by a rigid obstacle. A test case is proposed where an obstacle located at 1 cm in front of the vibrating structure is masking 45% of its surface. The remarkable quality of the reconstructed field compared to the reference computation demonstrates the capability of iPTF method to handle the presence of masking obstacles.

In addition, introduction of blind separation techniques in iPTF method should allow to distinguish velocity fields produced by different vibration sources. The last section is dedicated to show how the approach is used to separate the various phenomena that lead to the noise generation.

[1] emmanuel-manu.dabankah@insa-lyon.fr

2. THEORETICAL BACKGROUND OF THE IPTF METHOD

The following example in Figure 1 gives a brief description of iPTF method. Details of theoretical derivation have been presented in Ref. (3).

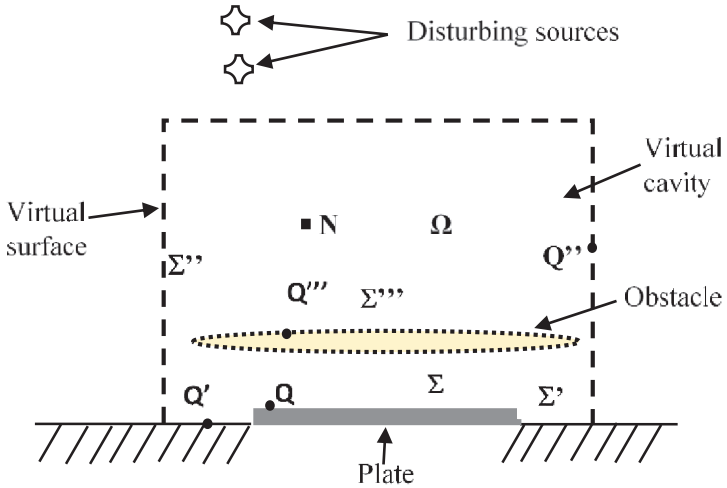

Figure 1 – Normal velocity reconstruction of a plate in a noisy environment in the presence of an obstacle

Let assume the source represented by the surface Σ vibrates with a known velocity field in a semi-infinite medium. The iPTF method is based on the definition of an arbitrary virtual acoustic cavity surrounding the source to identify (see Figure 1). The virtual acoustic cavity Ω engulfs an obstacle of surface Σ'''. This virtual cavity is thus delimited by the surfaces Σ', Σ'' and Σ''' with corresponding points Q', Q'' and Q''' (see Figure 1). Moreover, disturbing (stationary) sources might exist but must be excluded from the virtual cavity Ω. The acoustic problem is governed, in this acoustic domain, by the Helmholtz equation. On boundaries, a normal harmonic particle velocity $V_n e^{j\omega t}$ is imposed on the source surface, while the normal harmonic particle velocity $V_n^{rad} e^{j\omega t}$ on the virtual acoustic surface Σ'' results from the radiation of the source in the acoustic medium. The corresponding particle velocities on the obstacle surface Σ''' and platform surface Σ' are zero. This is because they are assumed to be rigid. Consequently, the virtual cavity problem to solve is given by Equation 1.

$$\begin{cases} \Delta p(N) + k^{*2} p(N) = 0 & \forall N \in \Omega \\ \dfrac{\partial p(Q)}{\partial n} = -j\omega\rho_0 V_n(Q) & \forall Q \in \Sigma \\ \dfrac{\partial p(Q')}{\partial n} = 0 & \forall Q' \in \Sigma' \\ \dfrac{\partial p(Q'')}{\partial n} = -j\omega\rho_0 V_n^{rad}(Q'') & \forall Q'' \in \Sigma'' \\ \dfrac{\partial p(Q''')}{\partial n} = 0 & \forall Q''' \in \Sigma''' \end{cases} \tag{1}$$

where Δ is the Laplacian operator, $\partial/\partial n$ the normal derivative outwardly directed, ω is the angular frequency, p is the acoustic pressure and k is the acoustic wavenumber. As detailed in Refs. (1-3), this system of equations can be solved introducing acoustic impedance transfer functions and dividing the surfaces into element surfaces called patches. Therefore, the pressure $p(N)$ at point N can be expressed as

$$p(N) = \sum_{j=1}^{N_m} Z_{Nj} \bar{V}_j + \sum_{l=1}^{N_s} Z_{Nl} \bar{V}_l \tag{2}$$

where

$$\begin{cases} Z_{Nj} = j\omega\rho_0 \sum_{n=1}^{\infty} \dfrac{\phi_n(N)\langle\phi_n\rangle_j A_j}{\Lambda_n(k^{*2} - k_n^2)} \\ Z_{Nl} = j\omega\rho_0 \sum_{n=1}^{\infty} \dfrac{\phi_n(N)\langle\phi_n\rangle_l A_l}{\Lambda_n(k^{*2} - k_n^2)} \end{cases} \tag{3}$$

The subscripts N, j and l denote respectively a point inside the virtual volume, a patch of the source surface Σ and a patch of the virtual surface Σ''. $\phi_n(N)$ are the mode shapes of the virtual cavity with rigid walls. Λ_n is the norm of the n-th mode shape. The notation $\langle X\rangle_l$ represents the space average of the variable X on patch l and A_l is the surface of the patch l. k_n is the real acoustic wavenumber at the eigen angular frequency ω_n, k^* is the complex wave number. The terms Z_{Nj} and Z_{Nl} are the acoustic impedances. Equation (2) permits the calculation of the pressure at a point N using the velocities of the patches. For a sake of simplicity, Equation 2 is rewritten under matrix form when handling several points i in the virtual cavity

$$\{P_i\} = [Z_{ij}]\{V_j\} + [Z_{il}]\{V_l\} \tag{4}$$

The aim of the iPTF method is to identify the source velocities $\{V_l\}$. For that purpose, one uses Equation 4, which after simple matrix manipulation allows to compute source velocities as

$$\{V_l\} = [Z_{il}]^{-1}\left(\{P_i\} - [Z_{ij}]\{V_j\}\right) \tag{5}$$

The acoustic patch impedance matrices of the volume defined by surfaces Σ and Σ'' are computed using Equation 3 and the eigenmodes extracted with a standard finite element solver. The pressure and velocity vectors of Equation 5 are measured in the virtual acoustic cavity Ω and on the virtual surface Σ'' respectively. The matrix $[Z_{il}]$ is often ill-conditioned and a regularization technique has to be used to invert it. The solution is found using Tikhonov regularization and the maximum of curvature of the L-curve is used to define the best regularization parameter – e.g. see Refs. (2, 4, 5).

3. NUMERICAL VALIDATION

For this numerical validation, the identification is performed on a simply supported plate excited by a harmonic point force as presented in Figure 2. The plate is 0.6m long, 0.4m wide, and 2mm thick, and it is made of aluminium (Young's modulus $E = 7.0 \times 10^{10}$ Pa; density $\rho = 2700$ kg/m^3; Poisson's ratio $\nu = 0.35$; damping $\eta = 0.01$). The plate is excited by a unit point force located at point (0.15; 0.15) m on the frequency band [100:500] Hz with frequency step of 25 Hz.

In the following example, the plate is partially masked by a rigid obstacle. As can be seen in Figure 2, this obstacle has an ovoid shape and is located really close to the plate (1 cm). This implies that no measurement can be done in this non-accessible zone. The aim of this example is to demonstrate that the iPTF method is able to handle the presence of an obstacle and still able to reconstruct the velocity field on the surface of the masked structure.

3.1 Measurement Step (Numerical Experiment)

To identify the source velocity field using the iPTF method, it requires measurement and numerical data. The measurement data are the set of pressure measurements taken randomly inside the virtual volume and the set of velocity measurements on the virtual surface patches. These measurements are usually done by physical experiments, but in present work they are simulated. The radiated field obtained at the measurement step has been provided by a numerical experiment performed using ACTRAN software (6).

The virtual acoustic surface Σ'' is made of the surfaces of a rectangular box (0.8 x 0.6 x 0.4) m open to the bottom. It is divided into 416 patches of size 0.05m. The plate is divided into 600 patches each of size 0.02 m. A set of 600 random field points are selected such that they are a least 0.02m from the surfaces of the source and virtual cavity. In all there were 416 velocity measurement points (in red) on the virtual surface and 600 pressure measurement points (in blue) in the acoustic cavity. The number of measurement points is voluntarily high to avoid questions raised by the use of an underdetermined problem. The obstacle is positioned between the source and these measurement points as shown in Figure 2. The pressure and velocity quantities are recorded from their corresponding field points as shown in Figures 3 and 4 respectively.

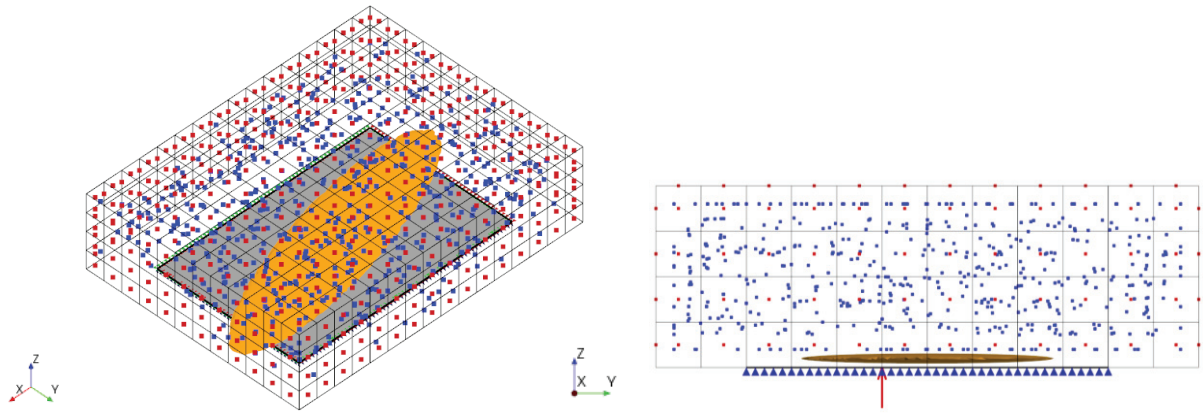

(a) (b)

Figure 2 – Geometric set up in ACTRAN software used in the acoustic radiation generation (blue points: field points in the virtual volume; red points: field points on the centroid position of the virtual surface patches; orange ovoid: obstacle; grey rectangle: plate; red arrow: point force; blue triangle: plate support; grid box: virtual surface patches). (a) 3D view; (b) Y-Z view.

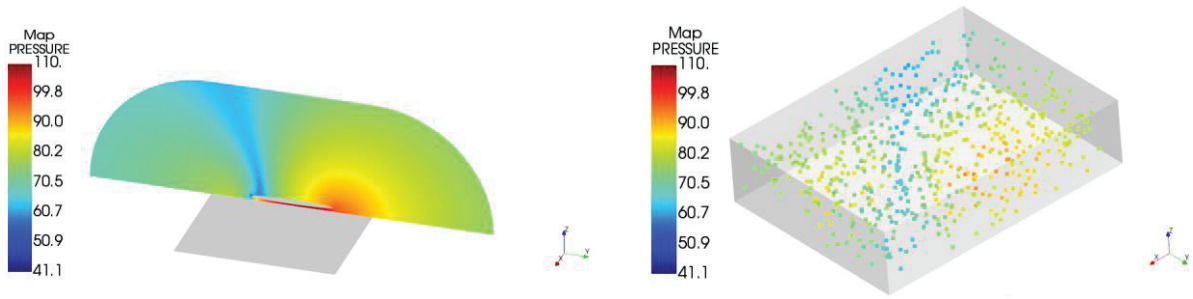

(a) (b)

Figure 3 – The radiated pressure (dB, ref = 2e-5 Pa) at 125Hz. (a) Y-Z section view of the acoustic radiated pressure field map. (b) Pressure field map of the random field points inside the virtual volume.

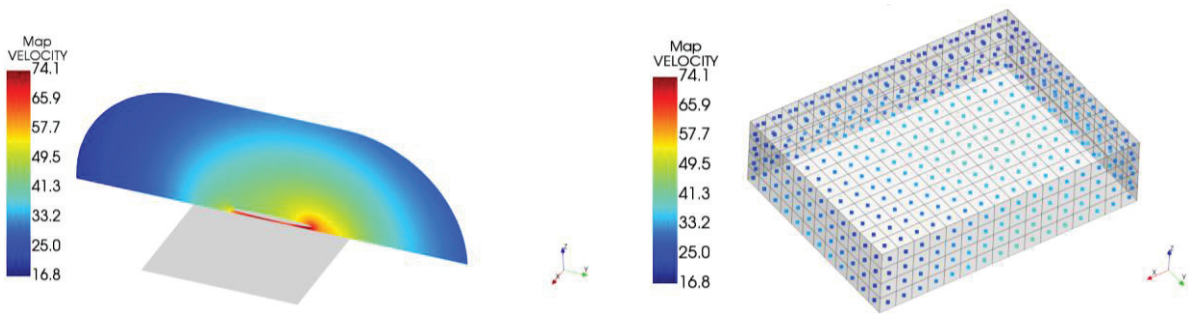

(a) (b)

Figure 4 – The acoustic particle velocity (dB, ref = 1e-9 m/s) at 100Hz. (a) the X-Z section view of the acoustic radiated velocity field map; (b) field map of the outward normal velocity acting on the centroids of the virtual surface patches.

The second set of data are the numerical data which are obtained by performing modal response analysis and finite element analysis of the virtual volume and its associated boundary surfaces (virtual surfaces and source surface) and the chosen random field points. The Neumann boundary condition is imposed on all boundary surfaces (2). This implies that the surrounding surfaces of the virtual cavity are assumed rigid. Obviously, this virtual cavity with rigid wall does not physically exist, it is only chosen for theoretical convenience as a basis for acoustic impedance decomposition (3). The eigen-modes of the virtual cavity with these rigid walls are computed up to 4250Hz (971 modes).

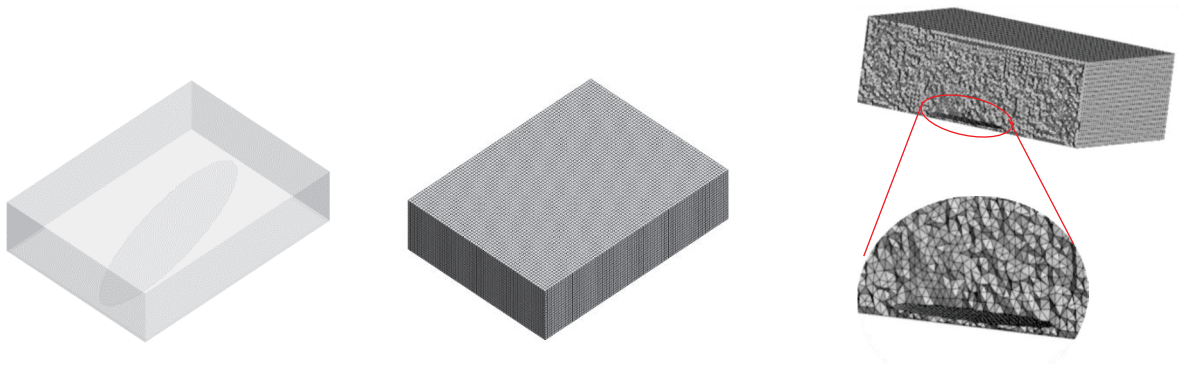

(a) (b) (c)

Figure 5 – Definition of the virtual acoustic cavity model. (a) unmeshed model of the virtual acoustic cavity; (b) 3D volume mesh of virtual acoustic cavity; (c) cut through of the virtual acoustic volume mesh revealing the position of the obstacle.

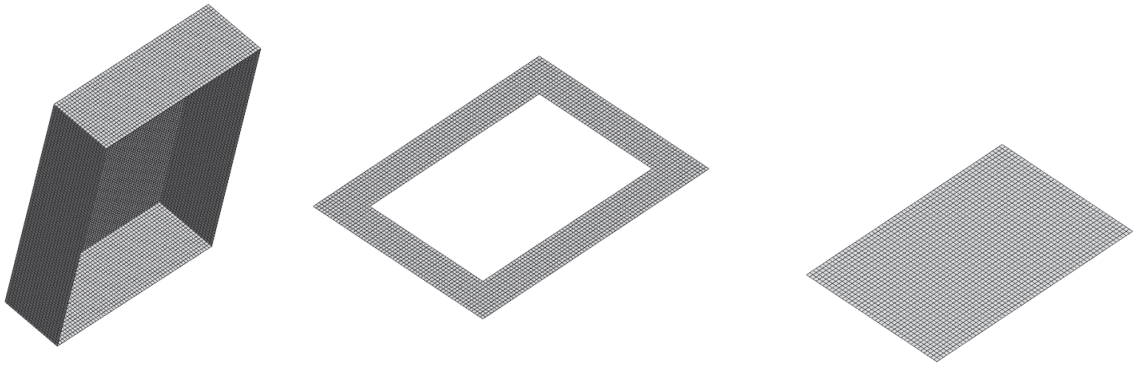

(a) (b) (c)

Figure 6 – Definition of the surfaces delimiting the virtual acoustic cavity used in the modal response analysis. (a) upper part of the 2D meshed virtual surface; (b) lower part of the 2D meshed virtual surface. (c) 2D surface mesh of the source.

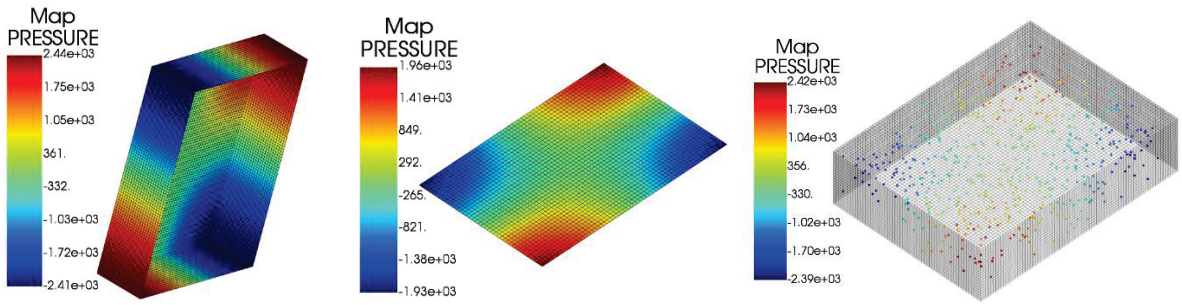

(a) (b) (c)

Figure 7 – The real part of the modal pressure maps at an eigenfrequency of 353Hz. (a) pressure map of the upper part of the 2D meshed virtual surface; (b) pressure map of 2D meshed source surface mesh; (c) the random field points inside the virtual volume.

3.2 Identification Step

The velocity field is identified using Equation (5) and the previously detailed data. It is important to note that the surface of identification corresponds to the surface of the plate, thus from the principle of continuity, the particle velocity is equal to the structural velocity of the plate. The computed plate and identified velocity fields are compared in terms of the norm velocity as presented in Figure 8. These results demonstrate that even in such an extreme case (45% of the structure is masked by a very close rigid object), the iPTF process can provide satisfactory results for this kind of blind identification.

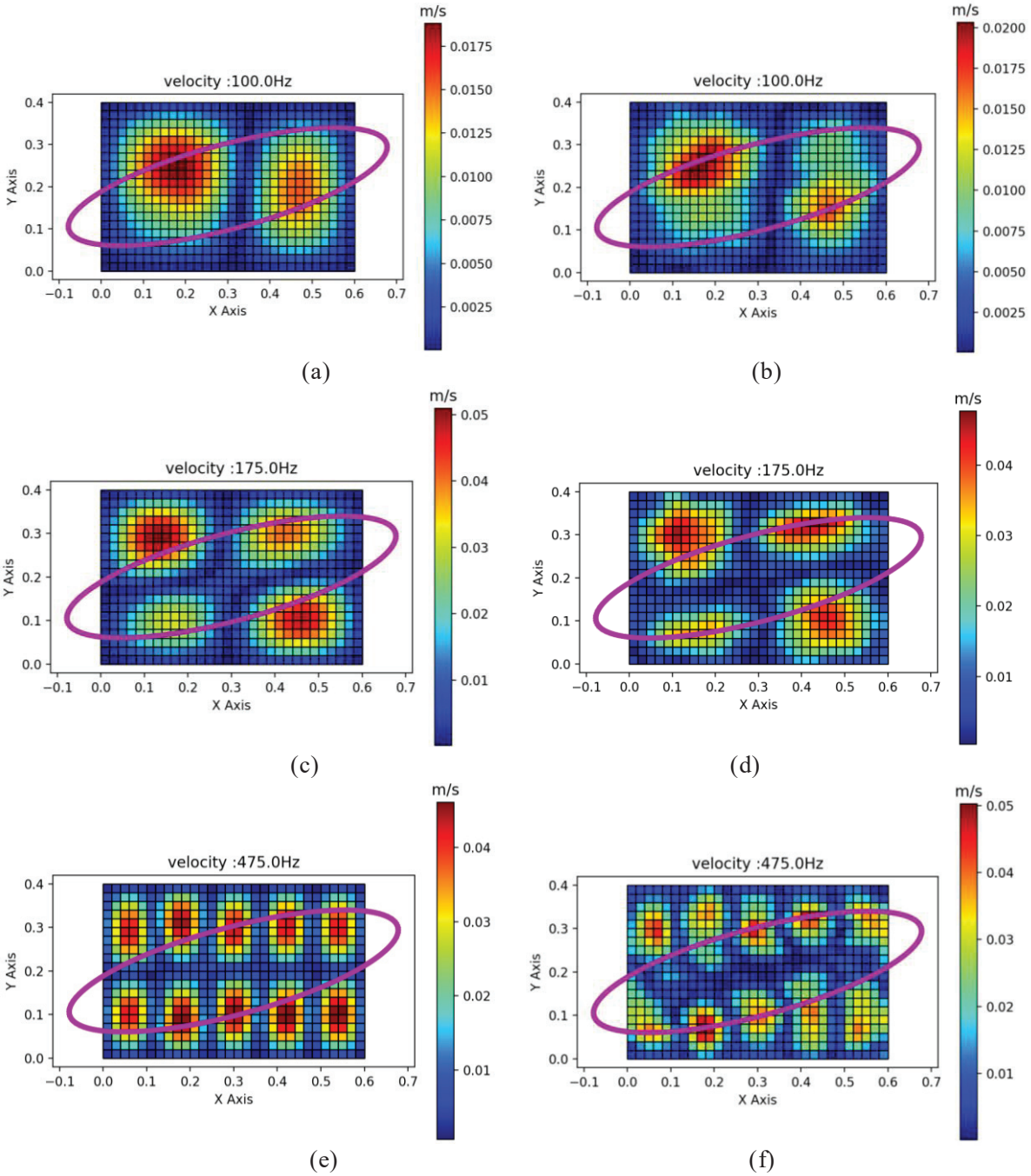

Figure 8 – The norm of the velocity field (a) computed on plate (reference) at 100Hz; (b) identified by iPTF at 100Hz; (c) computed on plate (reference) at 175Hz; (d) identified by iPTF at 175Hz; (e) computed on plate (reference) at 475Hz; (f) identified by iPTF at 475Hz. The tilted ellipse is the outline projection of the obstacle onto the plate.

4. SOURCE SEPARATION TECHNIQUES

In general, the iPTF method is able to identify radiated acoustic field based on phenomena leading to its generation. It is of interest to separate the partial contributions of the different phenomena that contribute to the overall radiated acoustic field. The phenomena in this context relates to the different sound sources (the mechanisms that lead to the excitation). A practical industrial example is the engine noise in a car. This radiated engine noise results from the mixture of many complex noises produced by various sources such as combustion, injection, compression and exhaustion. These are referred to as the phenomena. Pertaining to this work, the different phenomena will be blindly separated (which implies that there is no prior information about these phenomena). Some approaches, known as Blind

Source Separation (BSS) (7, 8) techniques will be evaluated in the context of iPTF method. BSS involves the task of 'blindly' recovering a set of unknown signals, the so-called sources from their observed mixtures, based on very little to almost no prior knowledge about the source characteristics or the mixing structure (9). The goal of BSS is to process multi-sensory observations of an inaccessible set of signals in a manner that reveals their individual (and original) form, by exploiting the spatial and temporal diversity, readily accessible through a multi-microphone configuration (8). Algebraically, most linear BSS models can be expressed as the following specific matrix factorization (10)

$$Y = AX + W \tag{6}$$

where Y is m×n observed mixture matrix, A is m×r mixing matrix, X is r×n source signal matrix, W is m×n noise signal matrix, and m, r and n stand for the number of observations, the number of sources, and the number of samples, respectively.

In present work, two ways to implement BSS are proposed. The first approach involves measuring acoustic field signals (particle velocities and pressure) with set of microphones directly from a vibrating structure. The measured acoustic data is used as the input Y, the observed mixture matrix. With the use of appropriate BSS method, X, the source signal matrix is retrieved. The second approach is similar to the CLEAN algorithm (11, 12) and an overview to this approach is illustrated in Figure 9.

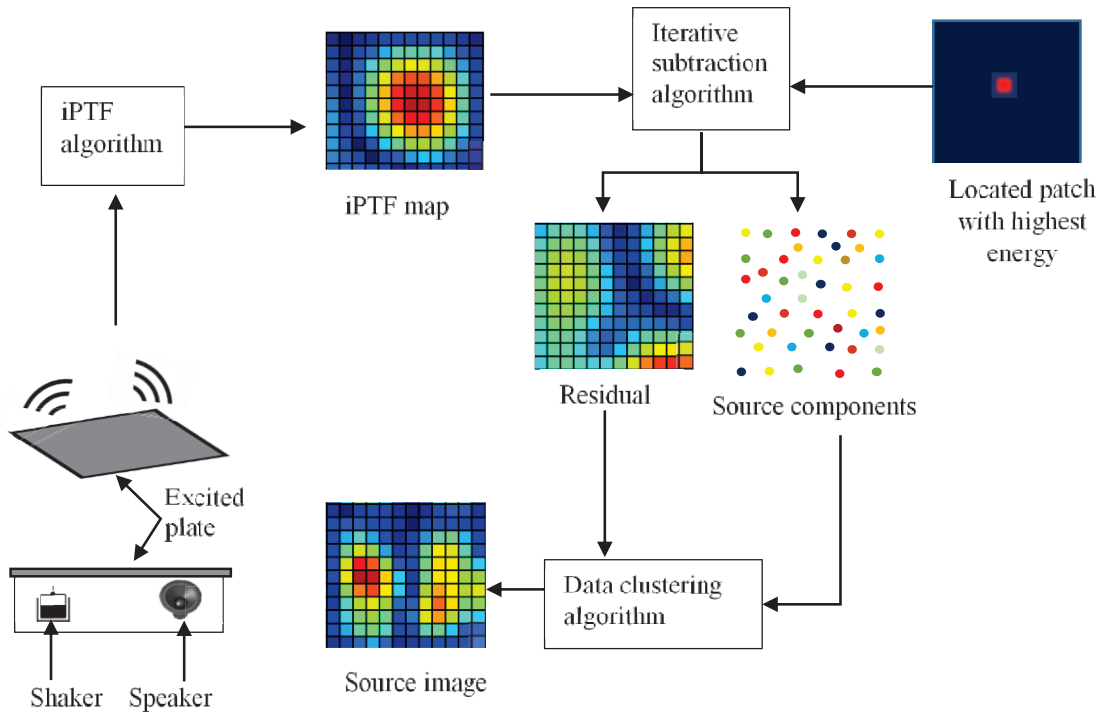

Figure 9 – Flowchart of the proposed separation algorithm routine with illustrative images. This is an image processing technique of the iPTF map.

The proposed algorithm aims to extract the sources using the iPTF velocity map and source prior information (sources coupling level and location). The iPTF velocity map can be viewed as a collection of patched sources. The quest is to recover the source image from the iPTF velocity map using a set of imaging processing techniques. The present sources are assumed to be spatially disjointed. The process begins with the identification of the patch with the highest energy level in the iPTF map. In an iterative process, this highest energy patch is subtracted from the iPTF velocity map. A delta function whose peak intensity and location equals highest energy patch (known as a source component) is saved to a separate image. What remains of the iPTF velocity map distribution (the 'residual' image) is fed back into the iterative loop and the cycle repeats until a stopping criterion is reached; usually a predetermined threshold value. By this method, the source components build up as a series of delta functions whose positions and intensities directly relate to the patched sources of iPTF velocity map. The source components and the residual image are combined using the k-means clustering algorithm (13) to generate the final source image.

5. CONCLUSIONS

In this article, iPTF has been used to identify velocity fields in the presence of obstacle. The main advantage of the method is the combined use of the integral formulation, FEM and measurements, which allows to overcome inherent limitations of classical methods. This paper gave an overview of the theoretical background and the numerical measurement methodology. To prove the method efficiency, a numerical validation was set up with a simple supported plate partially masked by a rigid obstacle. This identification has been compared to plate structural velocity. The results show a good comparison, which confirms the expected advantages, and demonstrate the applicability of the iPTF method.

The last part of the presented article presents a first thought on how to introduce blind source separation techniques in the context of iPTF method.

ACKNOWLEDGEMENTS

The authors gratefully acknowledge the European Commission for its support of the Marie Sklodowska Curie program through the ETN PBNv2 project (GA 721615).

This work was performed within the framework of the LABEX CeLyA (ANR-10-LABX-0060) of Université de Lyon, within the program « Investissementsd'Avenir » (ANR-16-IDEX-0005) operated by the French National Research Agency (ANR).

REFERENCES

1. Aucejo M., Totaro N., Guyader J.L., Identification of source velocities on 3D structures in non-anechoic environments: Theoretical background and experimental validation of the in-verse Patch Transfer Functions method. Journal of Sound and Vibration. 2010. 329; 3691-3708
2. Totaro N., Vigoureux D., Leclère Q., Lagneaux J., Guyader J.L. Sound fields separation and reconstruction of irregularly shaped sources. J. Sound Vib. 2015. 336; 62–81.
3. Forget S., Totaro N., Guyader J.-L., Schaeffer M., Source fields reconstruction with 3D mapping by means of the virtual acoustic volume concept. J. Sound Vib. 2016. 381;48-64.
4. Hansen P. C. Rank-Deficient and Discrete Ill-Posed Problems. SIAM. 1998. Philadelphia, PA.
5. Leclère Q. Acoustic Imaging Using Under-Determined Inverse Approaches: Frequency Limitations and Optimal Regularization .J. Sound Vib. 2009; 321(3–5): 605–619.
6. Actran 15.0 User's guide ,2018. Free Field Technologies SA.
7. Jutten C., Hérault J. Blind separation of sources, Part I: An adaptive algorithm based on neuromimetic architecture. Signal Processing. 1991; vol. 24, no. 1, pp. 1–10. DOI: 10.1016/0165-1684(91)90079-X.
8. Kostas Kokkinakis and Philipos C. Loizou. Advances in Modern Blind Signal Separation Algorithms: Theory and Applications. Synthesis Lectures on Algorithms and Software in Engineering. 2010; Vol. 2, No. 1, p. 1-100.
9. Comon P .Independent component analysis: A new concept. Signal Processing. 1994; vol. 36, no. 3, pp. 287–314. DOI: 10.1016/0165-1684(94)90029-9.
10. Cichocki A. Blind signal processing methods for analyzing multichannel brain signals. Int. J. Bioelectromagnetism. 2004.
11. Hogbom, J.A., "Aperture synthesis with a non-regular distribution of interferometer baselines", Astronomy and Astrophysics Supplement 15 (1974).
12. Taylor T.C, Hutchinson S., Salmon N. A., Wilkinsona N.P., Cameron C. D. Investigation of radio astronomy image processing techniques for use in the passive millimetre-wave security screening environment. 2014. Proc. of SPIE Vol. 9078, 90780J. DOI: 10.1117/12.2050574.
13. Lloyd S. Least squares quantization in PCM. IEEE Trans Inf Theory 1982;28(2):129–37.